Journal of Chromatography, 642 (1993) 459–467
Elsevier Science Publishers B.V., Amsterdam

CHROMSYMP. 2660

Determination of size and element composition distributions of complex colloids by sedimentation field-flow fractionation–inductively coupled plasma mass spectrometry

Deirdre M. Murphy

Water Studies Centre, Department of Chemistry, Monash University, 900 Dandenong Road, Caulfield East, Melbourne, Victoria 3145 (Australia)

John R. Garbarino and Howard E. Taylor

Division of Water Resources, US Geological Survey, Boulder, CO (USA)

Barry T. Hart and Ronald Beckett*

Water Studies Centre, Department of Chemistry, Monash University, 900 Dandenong Road, Caulfield East, Melbourne, Victoria 3145 (Australia)

ABSTRACT

Sedimentation field-flow fractionation (SdFFF) and inductively coupled plasma mass spectrometry (ICP-MS) have been directly combined and the resulting SdFFF–ICP-MS instrument can be used to produce element based size distributions of colloidal samples. Using appropriate tracer elements the size distributions of specific components can be picked out from a complex mixture. Changes in chemical composition of mixtures as a function of particle size can be readily monitored by plotting appropriate element atomic ratio distributions. These applications have been illustrated using data obtained with samples of the clay minerals kaolinite and illite and a natural suspended particulate matter from the Darling River (Australia).

INTRODUCTION

Colloid particles, which are often formally defined as being within the diameter range 1 nm to 1 μm, are extremely important in many industrial, biological and environmental processes. Consequently many methods have been developed in order to physically and chemically characterise these materials. Despite this, the sizing of polydisperse samples in the colloid range remains a difficult task with no single method proving to be totally adequate.

In analysing heterogeneous samples there are distinct advantages in using a technique that incorporates a preliminary separation step so that relatively monodisperse fractions are presented to the detection system. This is achieved with many methods based on transport properties, such as disc centrifugation. The problem is overcome in single particle counters (*e.g.*, Coulter counter, HIAC size analyser) by simply passing very dilute suspensions through the detector although the lower size for such methods is limited to about 0.5 μm by detector sensitivity. Elution methods such as field-flow fractionation (FFF) and hydrodynamic chromatogra-

* Corresponding author.

0021-9673/93/$06.00

phy have the additional advantages that narrow size range fractions can be collected at points across the distribution for subsequent observation and analysis. In the case of FFF this approach has been used quite extensively to establish if separation has occurred [1], confirm the calculated particle diameter [2], investigate particle morphology and mineralogy [3], determine particle density [4,5] and to study particle aggregation phenomena [6].

A particular focus in our research work has been the role of suspended colloids on the transport and fate of pollutants in natural waters [7]. These colloids are important due to their potentially high adsorption capacity and the fact that they generally remain suspended in fresh waters but aggregate and settle in saline waters such as during estuarine mixing. We have developed methods for applying sedimentation FFF (SdFFF) to size aquatic colloids [8]. In addition the high-resolution separations achieved have enabled detailed characterization of the size fractions using scanning electron microscopy, energy dispersive analysis of X-ray emissions [9], X-ray diffraction and inductively coupled plasma-emission spectrometry [3]. Beckett *et al.* [10] have introduced a methodology for investigating the adsorption behaviour of pollutants onto aquatic colloids. In these experiments SdFFF was used to separate the colloid particles after adsorption of a radiotracer labelled pollutant. The amount of adsorbent on the particles was determined by analysis of the eluent with a scintillation counter. Using the data it is possible to calculate the adsorption density distribution which gives the amount of pollutant adsorbed per unit particle surface area as a function of particle size.

A limiting factor with these analyses is the small amount of sample that can be processed in an FFF separation run. This means that only very sensitive analytical methods will be of use in characterizing the separated particle fractions. A preliminary set of experiments has been conducted using inductively coupled plasma mass spectrometry (ICP-MS) to analyse for selected elements [11]. A range of colloid samples, including a pigment, the minerals alumina and goethite and a river suspended particulate matter, were first separated by SdFFF and fractions of the eluent were collected and analysed by ICP-MS. This batch mode approach of combining SdFFF and ICP-MS has demonstrated that ICP-MS has a high enough sensitivity to detect even minor elements (*e.g.*, Mg) in the particles and that adsorption experiments with trace metal pollutants are feasible.

In this paper we report on the first experiments in which SdFFF and ICP-MS were directly coupled. The potential of SdFFF–ICP-MS is illustrated by the analysis of some clay minerals and suspended colloids from the Darling River (Australia). Ion response and element molar ratio distributions can be plotted which reflect the changes in mineralogy across the particle size distribution of the sample.

THEORY

Field-flow fractionation is a set of elution based separation and sizing methods which have been gaining wider use in recent years for characterizing a range of particles and macromolecules [12]. FFF is analogous to chromatography except that the separation mechanism is based on the physical interaction of sample particles with an applied field and the subsequent migration down the channel caused by the carrier fluid. In SdFFF the field is created by centrifugal acceleration as the thin unpacked channel is inserted inside a centrifuge basket (see Fig. 1). This causes sample components to accumulate at the outer wall of the channel where they form an equilibrium cloud whose mean thickness l depends on the buoyant mass of the particles (*i.e.*, size and density) and the field strength applied. Carrier flow in the thin flat channel is laminar with the linear fluid velocity being zero at the channel walls and increasing with distance away from each wall, thus approaching a maximum at the centre of the channel. Particles with larger effective mass will have more compressed sample clouds (smaller l) and will thus be swept down the channel by the carrier flow at a lower average velocity than smaller particles. The theory which describes this elution process has been described in detail elsewhere [8,12] and only the major equations that will be used here are summarised as follows.

For normal-mode FFF the retention ratio R, which is obtained from the measured elution volume V_r and channel void volume V^0, is related to the retention parameter λ by

$$R = \frac{V^0}{V_r} = 6\lambda\left(\coth\frac{1}{2\lambda} - 2\lambda\right) \quad (1)$$

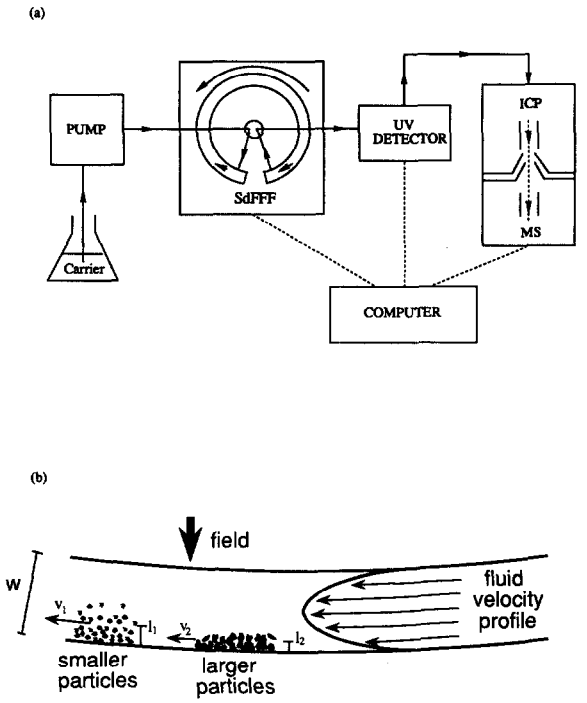

Fig. 1. Schematic representation of (a) the SdFFF–ICP-MS apparatus and (b) the SdFFF separation mechanism occurring in the channel.

where $\lambda = l/w$, with w being the channel thickness. In SdFFF runs at constant field strength the equivalent spherical particle diameter d can be calculated from λ provided the difference in density between the particle and carrier liquid $\Delta\rho$ is known

$$d = \sqrt[3]{\frac{6kT}{\pi\omega^2 rw\Delta\rho\lambda}} \tag{2}$$

where k is the Boltzmann constant, T the absolute temperature, ω the centrifuge speed (radians s^{-1}) and r the centrifuge radius.

Samples consisting of a broad size distribution require high field strengths for the resolution of the smaller particles. However, this may result in excessively long retention times for larger particles. To overcome this problem the field decay programming strategy of Williams and Giddings [13] was employed. This involved applying an initial constant speed ω_0 for a period t_1 after which the speed decayed according to the power equation

$$\omega = \omega_0 \left(\frac{t_1 - t_a}{t - t_a}\right)^4 \tag{3}$$

where t is the run time and t_a is a constant that controls the decay rate. If suitable values for ω_0, t_1 and t_a are chosen the fractionating power F_d [14] of the separation can be optimised to achieve a constant desired level of resolution across the entire size distribution.

The raw data obtained from a SdFFF instrument is usually a plot of detector signal *versus* elution volume (or time) and is referred to as a fractogram (*cf.*, chromatogram). The equivalent spherical particle diameter corresponding to a given elution volume can be computed employing eqns. 1 and 2 and assuming the run is made up of a large number of constant field increments stepping down from ω_0 as the field decays.

If the detector signal is proportional to the mass concentration of the sample in the eluent dm'_i/dV_i then the fractogram may be converted into a particle size distribution by plotting d on the x-axis and dm'_i/dd_i on the y-axis [10] where

$$\frac{dm'_i}{dd_i} \approx \frac{dm'_i}{dV_i} \cdot \frac{\delta V_i}{\delta d_i} \propto \text{detector signal} \cdot \frac{\delta V_i}{\delta d_i} \tag{4}$$

with m'_i being the mass of sample eluted up to point i of the digitised fractogram and δd_i is the change in d due to a very small increment in elution volume δV_i at point i. In most studies a UV detector is used to monitor the sample concentration although it is recognised that there will be some perturbation from the simple relationship between the measured absorbance level and eluent concentration due to the dependence of the signal on the particle size as the light attenuation is mostly due to scattering rather than absorption.

The SdFFF eluent was fed into an ICP-MS instrument which generates an ion current I_E for each element E of interest and I_E will be proportional to the mass concentration of the element (*i.e.*, dm'_{Ei}/dV_i). Thus in a similar manner the element based fractograms (*i.e.*, dm'_{Ei}/dV_i *versus* V_i) can be converted into element based size distributions (*i.e.*, dm'_{Ei}/dd_i *versus* d_i) [11] using

$$\frac{dm'_{Ei}}{dd_i} = \frac{dm'_{Ei}}{dV_i} \cdot \frac{\delta V_i}{\delta d_i} \propto I_{Ei} \frac{\delta V_i}{\delta d_i} \tag{5}$$

Furthermore data for different elements can be combined to give atom (or molar) ratio based size distributions which indicate very clearly any change in chemical composition across the size range of the sample.

EXPERIMENTAL

Sample preparation

RM30 is a sodium-saturated dithionite-treated illite with particle size less than 1 μm in diameter [15]. Purvis School Mine kaolinite was cut at approximately 0.5 μm by centrifugation to give two subsamples for analysis. The clay minerals were provided by Dr. D. Eberl from US Geological Survey, Denver, CO, USA. The solid concentration of clay dispersions injected into the SdFFF was about 5% (m/m).

The Darling River suspended particulate matter (SPM) was concentrated from raw river water by coagulation [8]. The method involved filtering the water through a Whatman GFC filter to remove large particulates and macroscopic debris, and then $CaCl_2$ was added to a concentration of 0.03 *M*. The solution was stirred then allowed to settle for 24 h during which time the aggregates settled. The supernatant was then syphoned from the vessel. Dionized water (Millipore Milli-Q) was added, the solution was stirred again, the allowed to settle as above. The procedure was repeated three times to wash the $CaCl_2$ from the suspension. The suspension was then sonicated to disaggregate and redisperse the sample. The density of both the clays and riverine SPM was assumed to be 2.5 g/ml. The final solids concentration in the suspension was about 1.2% (m/m).

SdFFF–ICP-MS apparatus

The SdFFF instrument used was the Model S101 fractionator from FFFractionation Inc. (Salt Lake City, UT, USA) and was similar to that described previously [11]. The channel void volume given by manufacturer was 4.93 ml. The channel width of 0.0283 cm was calculated using elution times from runs using polystyrene latex standards. The UV detector used was a Dionex UV–Vis detector operated at 254 nm. A Perkin-Elmer Series 100 pump was used to deliver carrier at 2.00 ml/min. The FFFractionation control and data acquisition program controlled and recorded the centrifuge speed, and recorded the UV signal.

The eluent from the SdFFF was delivered directly into a modified Sciex Elan Model 250 ICP-MS instrument operating with argon gas and equipped with a Babington-type pneumatic nebuliser. Analyte standards used included aluminium, magnesium, iron, strontium and rubidium at 100 μg/l, silicon dioxide at 500 μg/l, and calcium at 1000 μg/l. Internal standards used were rhodium, praseodymium and bismuth at 100 μg/l. ICP-MS data were collected by Perkin-Elmer software and this data analysed using FFFractionation and EXCEL spread sheet software. Standards were used to establish the specific sensitivity for each element and hence to determine the concentration of each element in the eluent from

$$\frac{dm'_{Ei}}{dV_i} = I_{Ei}(\text{sample}) \cdot \frac{\text{element concentration (standard)}}{I_E(\text{standard})} \quad (6)$$

The carrier was an aqueous solution of 1.00 g/l (0.0013 *M*) sodium pyrophosphate ($Na_4P_2O_7 \cdot$

TABLE I

SUMMARY OF SdFFF RUN CONDITIONS USED FOR EACH SAMPLE

Sample	Kaolinite 1 (<0.5 μm)	Kaolinite 2 (>0.5 μm)	Illite (RM30)	Clay mixture	Darling River SPM
Initial field (ω_0 RPM)	1500	150	1000	1000	1000
Holding field (ω_H RPM)	10	10	10	10	10
Time lag (t_l min)	7.28	12.95	8.057	8.057	10
Decay constant (t_a min)	−58.24	−103.6	−64.46	−64:46	−80
Fractionating power (F_d)	3	3	3	3	3.4

$10H_2O$, J. T. Baker) made up in water purified by a Barnsted NANOpure II system. The internal standards (Rh, Pr, Bi) were also added to the carrier. The sample injection volume for all the experiments using clay suspensions was 10 μl and for the Darling River SPM was 20 μl.

FFF run parameters

The field for each experiment was decayed according to the power program (eqn. 3) using the parameters listed in Table I. The FFF run parameters were chosen to yield a fractionating power F_d for the separation of about 3 [14,16]. A computer program written by P. S. Williams (University of Utah, Salt Lake City, UT, USA) was utilised in this calculation.

RESULTS AND DISCUSSION

Clay mineral samples

The fractograms generated for the two kaolinite samples (1 and 2) using the UV detector and the Al ion current from the ICP-MS are given in Fig. 2a and b. The normalised (total area = 1) particle size distributions computed from the fractograms utilising eqns. 4 and 5 are plotted in Fig. 2c and d. Although the <0.5 μm sample (kaolinite 1) has little material (5%) greater than the intended cutoff diameter of 0.5 μm the >0.5 μm sample (kaolinite 2) contained about 80% of material less than the nominal cutoff. This indicates that prior fractionation by centrifugation had provided a cut at about 0.35 μm but with some overlap in the distributions of the two subsamples.

The UV trace in the fractogram and consequently in the particle size distribution is shifted slightly to larger elution volume (and hence diameter) compared to the Al element curves. This is more pronounced with the smaller kaolinite 1 sample (<0.5 μm) and may be due to the dependence of the light scattering (and hence the intensity attenuation in the UV detector) on the particle size thereby causing a down weighting of the concentration of smaller particles in each sample.

The UV detector and Al ion current fractograms and particle size ditributions for the illite sample are given in Fig. 3. The shift in the UV detector response curves relative to those obtained by element analysis with ICP-MS are much more pronounced than for the kaolinite samples. This may be due to differences in the particle shape for the two minerals as scanning electron microscopy revealed that the illite consisted of very thin platelets and has a higher calculated aspect ratio than the kaolinite particles.

The element ion current data for the illite SdFFF run was converted to concentration (μg/l) using the

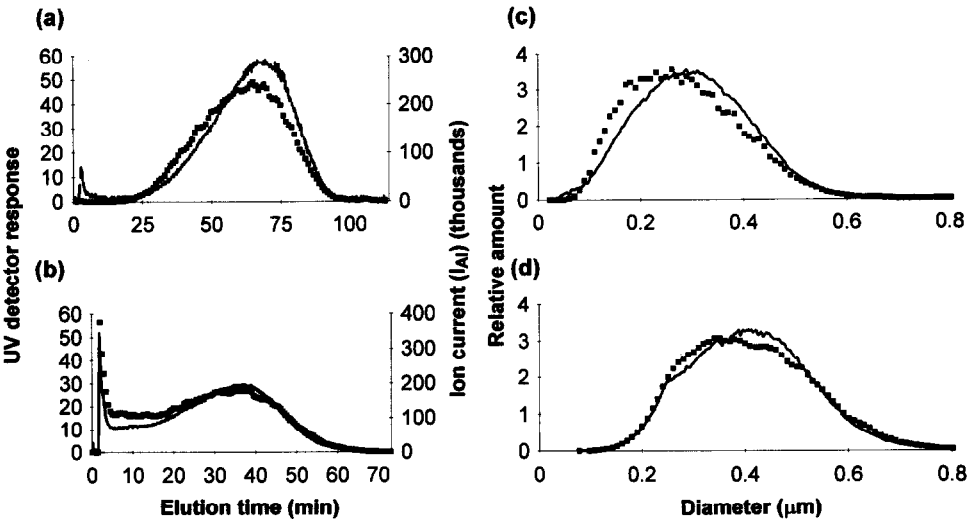

Fig. 2. Fractograms showing the SdFFF separations of Purvis School Mine kaolinite using the UV detector response (line) and Al ion current (squares) from the ICP-MS. (a) Kaolinite 1 (<0.5 μm), (b) kaolinite 2 (>0.5 μm). The corresponding size distributions calculated using the fractograms in (a) and (b) are also given. (c) Kaolinite 1 (<0.5 μm) and (d) kaolinite 2 (>0.5 μm).

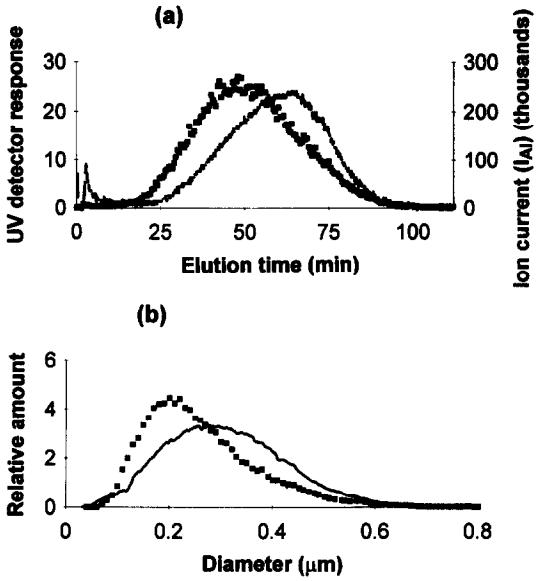

Fig. 3. (a) Fractograms showing the SdFFF separations of RM30 illite using the UV detector response (line) and Al ion current from the ICP-MS. (b) The calculated mass and Al-based size distributions obtained using the fractograms in (a). Line: UV response; squares: Al response.

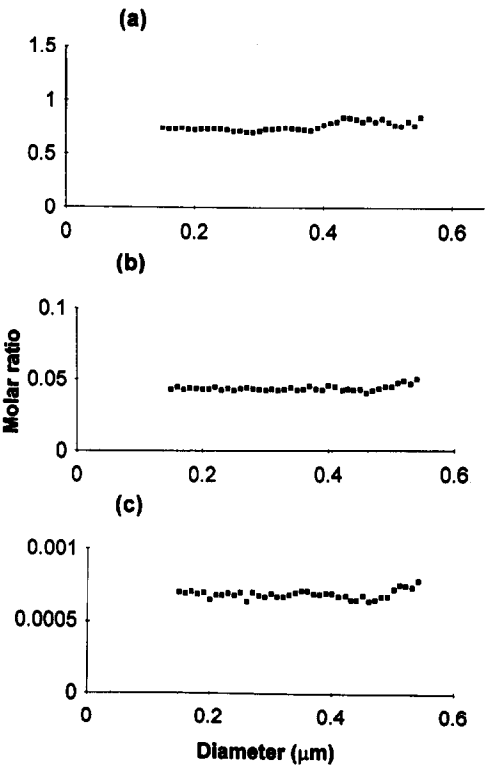

Fig. 4. Atomic ratio distributions (*i.e.*, element mol ratio *versus* particle diameter) for the illite sample (a) Si:Al, (b) Mg:Al and (c) Rb:Al.

element standard solutions (eqn. 6) and then the atomic ratio of selected elements compared to Al in the sample particles was calculated. The atomic ratios for Si:Al, Mg:Al and Rb:Al are plotted against particle size in Fig. 4. These atomic ratios are very constant across the entire size distribution showing that this illite sample has a uniform composition. The low Rb:Al atomic ratio of about $7 \cdot 10^{-4}$ shows that even trace elements can be detected in the solid samples.

The fact that Rb was present in the illite but was not detected in kaolinite suggests that suitable marker elements may be used to monitor the size distributions of certain components in a mixture. This is illustrated by the element based particle size distributions given in Fig. 5 which were obtained from fractograms of the individual illite and kaolinite 2 clays as well as a mixture of the two minerals. Thus Fig. 5a shows plots of the Al frequency function (*i.e.*, $dm'_{Al\,i}/dd_i$ from eqn. 5) for illite and kaolinite 2 and the Rb frequency function (*i.e.*, $dm'_{Rb\,i}/dd_i$) for illite. Each of these size distributions have been normalised to give a total area of 0.5 as the mixture contained equal masses of the two clays.

Fig. 5b gives the Al- and Rb-based particle size distributions for the mixture with the area under the Al curve being 1 since it reflects the total amount of illite and kaolinite whereas the area under the Rb curve is 0.5 as it represents only the illite component. By comparison with Fig. 5a it can be seen that the size distribution of illite has been accurately picked out from the clay mixture by monitoring the Rb ion response with ICP-MS. Also plotted in Fig. 5b is the sum of the Al curves for the individual illite and kaolinite 2 runs from Fig. 5a. This agreed quite well with the Al-based size distribution of the mixture despite the implied assumption that the Al content of both clays is the same (*cf.*, actual Al concentration of 20.9% for kaolinite and 17.5% for illite [15]).

Darling River SPM sample

Fig. 6a shows the fractograms for a suspended particulate matter sample collected from the Darling River (Australia) at Wentworth, N.S.W. just above

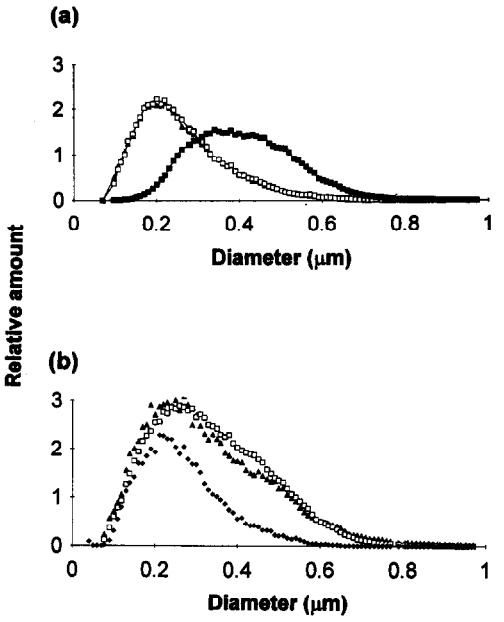

Fig. 5. (a) Individual clay separations: Al-based size distributions for illite (open squares) and kaolinite (>0.5 μm) (grey sqaures) and Rb-based size distribution for illite (triangles). All distributions normalized to have total area of 0.5. (b) Al- (▲) and Rb- (◆) based size distributions for a mixture of equal masses of the illite and kaolinite (>0.5 μm) clays. (Al area normalised to 1, Rb area normalised to 0.5). A summation of the Al responses for the individual clay curves is also shown (□).

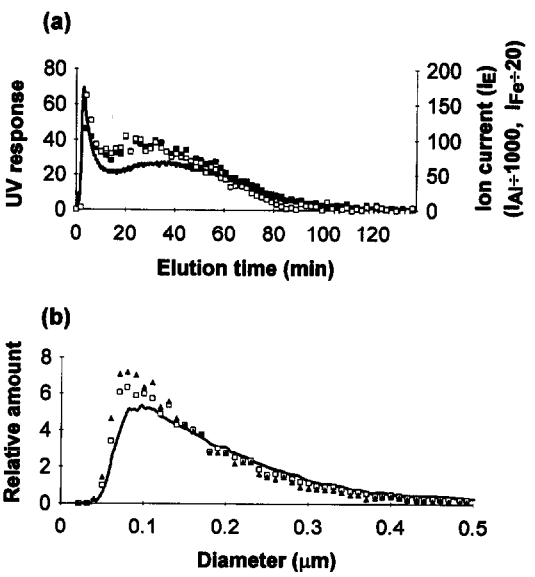

Fig. 6. (a) Fractograms showing the SdFFF separations of the Darling River SPM sample using the UV detector response and Al and Fe ion currents from ICP-MS. (b) The corresponding mass and element-based size distributions obtained using the fractograms in (a). Line: UV response; black squares or triangles: Al response; open squares: Fe response.

its confluence with the Murray River. The UV detector response as well as the Al and Fe ion currents measured by ICP-MS are plotted. The corresponding particle size distributions have been computed and are given in Fig. 6b. There appears to be general agreement between the UV and element based size distributions indicating that the light scattering shift in the UV-based size distribution, so apparent in the illite clay data, is not significant with this SPM sample.

Some knowledge of the mineralogical composition of the Darling River SPM has been attained with X-ray powder diffractometry and elemental analysis on the bulk sample [17]. The major minerals present are illite 15%, kaolin 22%, smectite 48% and quartz 15%. More detailed information on the size ranges of the mineral phases should be feasible using SdFFF–ICP-MS. An excellent method for examining these trends in mineralogy across the size distribution of a sample is to plot the relevant element atomic ratios as a function of the equivalent spherical diameter as illustrated by the graphs in Fig. 7.

The Si:Al atomic ratio plotted in Fig. 7a shows an almost constant ratio for the smaller particles (0.08–0.25 μm) followed by a pronounced increase which results in a doubling of the atomic ratio over the size range from 0.25 to 0.45 μm. A feasible explanation for this trend in Si:Al atomic ratio may be an increase in the proportion of silica (SiO_2) compared to the clay minerals as the size increases. Alternatively it could be caused by a change in the relative amounts of kaolin, illite and smectite minerals as particle size increases, since smectite in particular has a much higher Si:Al ratio. At present we have no independent evidence for the exact mineralogical changes occurring across the size range in these samples but this could be provided by more detailed characterization (*e.g.*, diffraction measurements) of the fractions produced by SdFFF [3].

The Mg:Al atom ratio (Fig. 7b) decreases significantly with increased particle size. Since Mg is probably present as isomorphous replacement ions in the clay lattice or in interlayer cation exchange

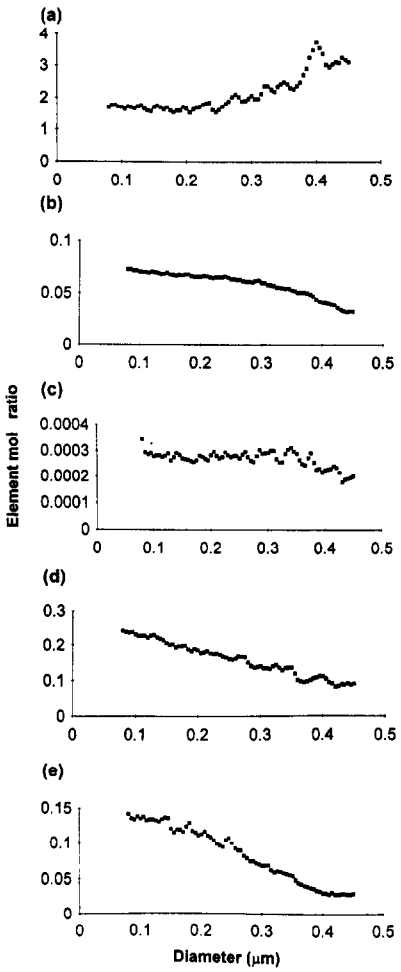

Fig. 7. Atomic ratio distributions (*i.e.*, element mol ratio *versus* particle diameter) for the Darling River SPM sample. (a) Si:Al, (b) Mg:Al, (c) Rb:Al, (d) Fe:Al and (e) Fe:Si.

positions this trend suggests some change in clay mineralogy is occurring with particle size. Furthermore the most likely explanation would be a decrease in illite and smectite (as opposed to a possible increase suggested above) as one would expect silica or kaolin to have the lowest Mg content of the minerals present. This supports the hypothesis that the proportion of silica increases substantially with particle size thus resulting in an over all increase in the Si:Al ratio rather than the alternative explanation of an increase in the smectite and illite clays with particle size.

In contrast the Rb:Al ratio is almost constant over the whole size range (Fig. 7c). Thus Rb and Mg are not present in the same proportion in all of the minerals present which is not unexpected as Rb is more likely to be a replacement for K or Na in clays.

The Fe:Al mole ratio plotted in Fig. 7d shows a small but steady decrease over the entire size range (0.08–0.45 μm). A decrease in Fe content as particle size increases would be anticipated if a significant amount of iron were in the form of surface coatings of hydrous iron oxides. Minerals with high Fe:Al ratios such as illite or smectite may also contribute to the trend in Fe content if they are present in larger amounts in the smaller size ranges. All the element atomic ratios with Si show substantial downward trend with increase in particle size. For example the Fe:Si ratio shown in Fig. 7c decreases by a factor of 3 over the range 0.08 to 0.45 μm. The most likely explanation is the dilution of the element concentrations by the increasing amount of silica rather than the alternative proposition of an increase in the smectite and illite clays with particle size.

CONCLUSIONS

This study has demonstrated that SdFFF can be interfaced directly with ICP-MS to produce element composition data across the size distribution of colloidal samples. Data collected with the clay minerals koalinite and illite have shown that both major and minor elements can be detected. If a suitable tracer element is present then the size distribution of one component can be picked out from a mixture. For complex samples changes in composition as a function of particle size can be conveniently monitored using plots of atomic ratio *versus* particle size for appropriate elements. This approach was illustrated with data for a suspended particulate matter sample collected from the Darling River (Australia).

Previous work on SdFFF and ICP-MS, in the rather more laborious fraction collection and sample analysis batch mode of operation, has demonstrated that SdFFF–ICP-MS will be a valuable method for studying adsorption behaviour [11]. This could include generating adsorption density distributions which show the trend in amount adsorbed per unit particle surface area as a function of particle diameter [10]. Future work should expand the range

of elements analysed as well as check for sample matrix and particle size effects on the raw ion currents produced by the ICP-MS.

The size range covered by the current SdFFF–ICP-MS instrument is about 0.05–2 μm although it has been proposed that this could be expanded by using other subtechniques of FFF [18]. Thus flow FFF could be used for very fine colloids (< 0.05 μm) and even macromolecules down to about 1000 dalton in molecular mass. The hyperlayer or steric mode of FFF operation could be used for larger silt sized particles (> 2 μm), however, in this range the effect of particle size on the degree of atomization and ionization of the elements by the ICP torch would need to be carefully tested.

The FFF–ICP-MS method shows great potential for the detailed physical and chemical characterisation of complex mixtures.

ACKNOWLEDGEMENTS

One of us (D.M.M.) was supported by an Australian Postgraduate Research Award and this collaboration with the US Geological Survey, Denver, CO, USA, was made possible by a Royal Australian Chemical Institute Parfitt-Iler Award and a Monash University Travel Grant. The FFF research program in Australia was supported by the Australian Research Council and the Land and Water Resources Research and Development Corporation.

The use of tradenames does not imply endorsement by the US Geological Survey.

REFERENCES

1 R. Beckett, *Environ. Technol. Lett.*, 8 (1987) 339–354.
2 S. K. Ratanathanawongs and J. C. Giddings, *J. Chromatogr.*, 467 (1989) 341–356.
3 D. J. Chittleborough, D. M. Hotchin and R. Beckett, *Soil Sci.*, 153 (1992) 341–348.
4 R. V. Sharma, R. T. Edwards and R. Beckett, *Appl. Environ. Microbiol.*, submitted for publication.
5 K. D. Caldwell and J. Li, *J. Colloid Interface Sci.*, 132 (1989) 256–268.
6 B. N. Barman and J. C. Giddings, *Langmuir*, 8 (1992) 51–58.
7 B. T. Hart (Editor), *Water Quality Management: The Role of Particulate Matter in the Transport and Fate of Pollutants*, Water Studies Centre, Melbourne, 1986.
8 R. Beckett, G. Nicholson, B. T. Hart, M. E. Hansen and J. C. Giddings, *Water Res.*, 22 (1988) 1535–1545.
9 R. Beckett, G. Nicholson, D. M. Hotchin and B. T. Hart, *Hydrobiologia*, 235/236 (1992) 697–710.
10 R. Beckett, D. M. Hotchin and B. T. Hart, *J. Chromatogr.*, 517 (1990) 435–447.
11 H. E. Taylor, J. R. Garbarino, D. M. Murphy and R. Beckett, *Anal. Chem.*, 64 (1992) 2036–2041.
12 J. C. Giddings, *C&E News*, 66 (1988) 34–45.
13 P. S. Williams and J. C. Giddings, *Anal. Chem.*, 59 (1987) 2038–2044.
14 J. C. Giddings, P. S. Williams and R. Beckett, *Anal. Chem.*, 59 (1987) 28–37.
15 D. D. Eberl, J. Srodon, M. Lee, P. H. Nadeau and H. R. Narthrop, *Am. Mineral.*, 72 (1987) 914–934.
16 P. S. Williams, L. Kellner, R. Beckett and J. C. Giddings, *Analyst*, 113 (1988) 1253–1259.
17 G. Douglas, unpublished results, 1990.
18 R. Beckett, *At. Spectrosc.*, 12 (1991) 228–232.